

On measurement of top polarization as a probe of $t\bar{t}$ production mechanisms at the LHC

Rohini M. Godbole,^{a,1} Kumar Rao,^b Saurabh D. Rindani^c and Ritesh K. Singh^d

^aTheory Unit, CERN,
CH-1211, Geneva 23, Switzerland

^bDepartment of Physics, University of Helsinki and Helsinki Institute of Physics,
P.O. Box 64, FIN-00014, Helsinki, Finland

^cTheoretical Physics Division, Physical Research Laboratory,
Navrangpura, Ahmedabad 380 009, India

^dInstitut für Theoretische Physik und Astronomie, Universität Würzburg,
Würzburg, 97074, Germany

E-mail: rohini@cts.iisc.ernet.in, saurabh@prl.res.in,
singh@physik.uni-wuerzburg.de

ABSTRACT: In this note we demonstrate the use of top polarization in the study of $t\bar{t}$ resonances at the LHC, in the possible case where the dynamics implies a non-zero top polarization. As a probe of top polarization we construct an asymmetry in the decay-lepton azimuthal angle distribution (corresponding to the sign of $\cos\phi_\ell$) in the laboratory. The asymmetry is non-vanishing even for a symmetric collider like the LHC, where a positive z axis is not uniquely defined. The angular distribution of the leptons has the advantage of being a faithful top-spin analyzer, unaffected by possible anomalous tbW couplings, to linear order. We study, for purposes of demonstration, the case of a Z' as might exist in the little Higgs models. We identify kinematic cuts which ensure that our asymmetry reflects the polarization in sign and magnitude. We investigate possibilities at the LHC with two energy options: $\sqrt{s} = 14$ TeV and $\sqrt{s} = 7$ TeV, as well as at the Tevatron. At the LHC the model predicts net top quark polarization of the order of a few per cent for $M_{Z'} \simeq 1200$ GeV, being as high as 10% for a smaller mass of the Z' of 700 GeV and for the largest allowed coupling in the model, the values being higher for the 7 TeV option. These polarizations translate to a deviation from the standard-model value of azimuthal asymmetry of up to about 4% (7%) for 14 (7) TeV LHC, whereas for the Tevatron, values as high as 12% are attained. For the 14 TeV LHC with an integrated luminosity of 10 fb^{-1} , these numbers translate into a 3σ sensitivity over a large part of the range $500 \lesssim M_{Z'} \lesssim 1500$ GeV.

KEYWORDS: Beyond Standard Model, Heavy Quark Physics, Standard Model

ARXIV EPRINT: [1010.1458](https://arxiv.org/abs/1010.1458)

¹Permanent address: Center for High Energy Physics, Indian Institute of Science, Bangalore 560 012, India.

Contents

1	Introduction	1
2	Model and calculational framework	3
3	Results	7
3.1	Top polarization	8
3.2	Lepton azimuthal distribution	10
3.3	Kinematic cuts for A_ℓ	13
3.4	Statistical significance of δA_ℓ	16
3.5	The role of kinematic cuts	17
3.6	Results for lower energy colliders: the Tevatron and LHC with $\sqrt{s} = 7$ TeV	19
4	Conclusions	21

1 Introduction

The properties and interactions of quarks and leptons belonging to the third family are still relatively poorly known. Universality of interactions of all the three generations is a natural prediction of the Standard model (SM), but the number of generations and the relative masses in the model seem completely ad hoc. Serious constraints have been set on the universality of couplings of the first two generations, but for the third, it is less well tested. The closeness of the top quark mass to the Electroweak symmetry breaking (EWSB) scale, in fact, leads to speculations that it might be closely related to an answer to the as yet unsolved problem of the EWSB and alternatives to the SM Higgs mechanism almost always involve the top quark [1]. Most of the Beyond the Standard Model (BSM) scenarios have a new particle which is closely related to the top quark in one way or the other and hence the top quark always plays an important role in BSM searches at colliders: be it the supersymmetric partner of the top (the stop) [2, 3] or the heavy top expected in the Little Higgs models [4, 5]. In addition, many BSM models also predict strongly coupled $t\bar{t}$ resonances, with or without preferential couplings to a $t\bar{t}$ pair [4–10]. Clearly, one expects a top factory such as the LHC to be an ideal place to hunt for BSM physics in top production [11–14]. Already at the Tevatron, the study of top physics has proved quite fruitful with combined fits providing constraints on masses and production cross-sections of $t\bar{t}$ resonances [15–18] as well as from consideration of their contribution to the total $t\bar{t}$ cross-section [19, 20]. The observation of a forward-backward asymmetry [21, 22] in $t\bar{t}$ production, differing from the SM expectation at more than 2σ level, is perhaps one of the few ‘disagreements’ between the experimental data and the SM predictions and has found a host of BSM explanations.

With a large mass of about 175 GeV, the top quark has an extremely short lifetime, calculated in the SM to be $\tau_t = 1/\Gamma_t \sim 5 \times 10^{-25}$ second. This is an order of magnitude smaller than the hadronization time scale, which is roughly $1/\Lambda_{\text{QCD}} \sim 3 \times 10^{-24}$ second. Thus the top decays before it can form bound states with lighter quarks. As a result the kinematical distribution of its decay products retain the memory of the top spin direction. Clearly, top spin information holds more clues to top production dynamics than just the cross-section. For example, in the MSSM, the expected polarization of the top produced in the decay of the stop can provide information on model parameters such as mixing in the neutralino/sfermion sector or amount of CP violation [23, 24]. Use of top polarization as a probe of additional contributions to $t\bar{t}$ production due to sfermion exchange in R-parity violating MSSM, was suggested in ref. [25]. It is interesting to note that this would also imply a forward-backward asymmetry in top production such as reported at the Tevatron. Thus in this case top polarization may be able to provide a discrimination between different explanations that have been put forward. More generally, top polarization can offer separation between different processes responsible for top production [26] or can allow discrimination between different BSM models with differing spins of the top partner [27, 28].

Probing BSM dynamics in top physics can thus receive an additional boost if top polarization or $t\bar{t}$ spin-spin correlations can be faithfully inferred from the kinematic distributions of its decay products. For example, expected kinematic distributions of the decay products of the top have been used to fine tune search strategies for BSM physics such as the top partner in Little Higgs models or the Kaluza-Klein (KK) gluons expected in brane-world models with warped extra dimensions [29–31]. The large Yukawa coupling of the t quark with the Higgs boson makes it an ideal candidate for studying properties of the Higgs boson, particularly so because it can offer a way to distinguish between the chirality conserving gauge interactions and chirality flipping Yukawa interactions. In fact, the final state top quark polarization for associated $t\bar{t}H$ production in e^+e^- collisions can reflect the CP-parity of the Higgs boson [32]. For hadronic $t\bar{t}$ production, spin-spin correlations between the decay leptons from the t and \bar{t} have been extensively studied in the SM and for BSM scenarios [11, 33–39]. These spin-spin correlations measure the asymmetry between the production of like and unlike helicity pairs of $t\bar{t}$ which can probe new physics in top pair production. Correlations between the spins of t, \bar{t} produced in the decay of the Higgs or in association with the Higgs, also reflect the spin-parity of the Higgs boson [12]. Strategies have been outlined for using these correlations for studying KK graviton excitations [40] as well. However, measuring spin correlations requires the reconstruction of the t and \bar{t} rest frames, which is difficult, if not impossible, at the LHC. In this note we wish to explore use of *single top polarization* as a qualitative and quantitative probe of new physics in $t\bar{t}$ production, keeping in mind that it would offer higher statistics compared to studies of spin-spin correlations.

As has been noted already, most of the spin studies mentioned here and various suggestions for similar studies always involve the construction of observables in the rest frame of the decaying top quark. It would be interesting and useful to construct observables to track the decaying top quark polarization using kinematic variables in the laboratory

frame. It is well known that the angular distribution of a decay fermion, measured with respect to the direction of the top spin in the rest frame of the top quark, can be used as a top spin analyzer, the lepton being the most efficient analyzer. This angular distribution translates into specific kinematic distributions for the decay lepton in the laboratory frame where the t is in motion, depending on the polarization of the decaying quark. However, it is the energy averaged angular distribution of the decay lepton which is found to be independent of any possible anomalous contribution to the tbW vertex [41–49]. If the dynamics gives rise to net polarization of the decaying top quark, at a collider like the Tevatron this can translate into a polarization asymmetry with respect to the beam direction and hence an asymmetry in the decay lepton angular distribution with respect to (say) the proton direction in the laboratory. However, at a collider like the LHC, where the direction of either proton can be chosen to be the positive direction of the z axis, simple observables like this will vanish even if the dynamics gives rise to a polarization asymmetry for the top (and hence an angular asymmetry of the decay lepton in the laboratory) with respect to the direction of one of the protons. Hence, it is necessary to construct a non-vanishing observable which will faithfully reflect such non-zero polarization.

In this note we address the issue of constructing such an observable at the LHC which would serve as a faithful measure of the polarization of the top quark arising from the dynamics of the subprocess of production. We show that it is possible to construct an asymmetry, measured in the laboratory frame, using the distribution in the azimuthal angle of the decay lepton with respect to the $x - z$ plane, being the plane containing the direction of one of the protons as the z axis and the direction of the decaying t quark. This observable directly reflects the sign and the magnitude of the t polarization, with a suitable choice of kinematic cuts. We demonstrate this using as an example the production of a $t\bar{t}$ resonance, with chiral couplings to the fermions, as in the Littlest Higgs Model [4, 5]. A preliminary study of the possibility of using this observable and hence the top polarization to get information on the structure of couplings of these resonances with the t/\bar{t} , has been presented elsewhere [31, 50, 51].

In section 2 we present the details of the model as well as the calculational framework. In section 3 we present results. We begin by showing our results for t polarization at the LHC, both for $\sqrt{s} = 14$ and 7 TeV, for Z' production with chiral couplings expected in the Littlest Higgs Model, over the parameter space of the model, with and without integration over the invariant mass of the $t\bar{t}$ pair. We then describe the construction of the azimuthal angle asymmetry in the laboratory frame as a measure of the t polarization. Next we show its dependence on the kinematic variables in the problem. This then help us identify the kinematic cuts, such that this asymmetry reflects the size and the sign of the t polarization faithfully. We then present our results on the sensitivity of the LHC at 14 and 7 TeV, as well as that for the Tevatron, for the Z' model under consideration and then conclude.

2 Model and calculational framework

There exist various examples of $t\bar{t}$ resonances in different BSM scenarios; the strongly interacting ones, like KK gluons, colorons, axigluons, as well as various other versions of

additional Z' resonances (for a review, see [52]) that occur in almost all the BSM scenarios, with a variety of couplings to different fermions. In the former case of strongly interacting resonances, there are two classes, one with enhanced couplings to $t\bar{t}$ pair which includes KK gluons and the other without such enhanced couplings, which includes colorons, axigluons etc. Search for additional Z' in the leptonic channel is an item with high priority on the agenda of the LHC first run [53–55]. In the leptonic channel, even with the 1 fb^{-1} luminosity and lower centre of mass energy of 7 TeV, the LHC in this first run should be able to probe beyond the current Tevatron limits [56]. Since couplings to the third generation of fermions could be substantially different in different models, even if we are blessed with an early discovery of a Z' in the leptonic channel at the LHC, a clear and complete characterization of such a resonance and hence the BSM physics it may correspond to, will require determination of these. A Z' with a chiral coupling to $t\bar{t}$ would give rise to substantial polarization of the top, which could be a distinguishing feature of the model. Here we illustrate how azimuthal distributions can be used to investigate top polarization, using the example of a Z' with purely chiral couplings, such as the one that occurs in a model similar to the Littlest Higgs model.

We consider a Z' of mass $M_{Z'}$ whose couplings to quarks are purely chiral, given by [57]

$$\mathcal{L}_{q\bar{q}Z'} = -\frac{1}{2}g \cot(\theta) \sum_{i=1}^3 [\bar{u}_i \gamma_\mu P_{L,R} u_i - \bar{d}_i \gamma_\mu P_{L,R} d_i] Z'^\mu, \quad (2.1)$$

where g is the weak coupling constant and $\cot(\theta)$ is a free parameter in the model. The subscripts $P_{L,R}$ refer respectively to left- and right-chiral projection operators. If Z' is Z_H of the Littlest Higgs model, we would choose the subscript L in the above equation. However, we will also use for illustration a model in which Z' has pure right-chiral couplings, for which we choose the subscript R . With the couplings of eq. (2.1), the total decay width of Z' comes out to be

$$\Gamma_{Z'} = \frac{g^2}{96\pi} M_{Z'} \cot^2(\theta) \left[21 + 3\sqrt{1 - 4m_t^2/M_{Z'}^2} (1 - m_t^2/M_{Z'}^2) \right], \quad (2.2)$$

where the partial decay widths into W^+W^- and ZH have been neglected [57]. Since the dominant production mechanism for $t\bar{t}$ in the SM is parity-conserving, top polarization expected in the SM is very small, both at the Tevatron and the LHC. However, a Z' with chiral couplings as given by eq. (2.1) can give rise to substantial top and anti-top polarization, for sufficiently large values of $\cot(\theta)$ and for values of $m_{t\bar{t}}$ comparable to $M_{Z'}$. The kinematic distribution of the decay fermions coming from the t or \bar{t} can be used to get information on this polarization. Below we first discuss how this is accomplished in the rest frame of the decaying top and also sketch out the necessary formalism used to calculate the correlated production and decay of the top keeping the spin information.

The angular distribution of the decay products of the top is correlated with the direction of the top spin. In the SM, the dominant decay mode is $t \rightarrow bW^+$, with the W^+ subsequently decaying to $l^+\nu_\ell$, $u\bar{d}$ or $c\bar{s}$, with l denoting any of the leptons. For a top quark ensemble with polarization P_t , in the top rest frame the angular distribution of the

decay product f (denoting W^+ , b , l^+ , ν_ℓ , u and \bar{d}) is given by,

$$\frac{1}{\Gamma_f} \frac{d\Gamma_f}{d \cos \theta_f} = \frac{1}{2} (1 + \kappa_f P_t \cos \theta_f). \quad (2.3)$$

Here θ_f is the angle between the decay product f and the top spin vector in the top rest frame, and the degree of top polarization P_t for the ensemble is given by

$$P_t = \frac{N_\uparrow - N_\downarrow}{N_\uparrow + N_\downarrow} \quad (2.4)$$

where N_\uparrow and N_\downarrow refer to the number of positive and negative helicity tops respectively. Γ_f denotes the partial decay width. κ_f is a constant which depends on the weak isospin and the mass of the decay product f and is called its spin analyzing power. Obviously, a larger value of κ_f makes f a more sensitive probe of the top spin. At tree level, the charged lepton and d anti-quark are thus best spin analyzers with $\kappa_{l^+} = \kappa_{\bar{d}} = 1$, while $\kappa_{\nu_\ell} = \kappa_u = -0.31$, with $\kappa_b = -\kappa_{W^+} = -0.41$. Eq. (2.3) thus tells us that the l^+ or d have the largest probability of being emitted in the direction of the top spin and the least probability in the direction opposite to the spin. Since among these two it is the charged lepton (l^+) for which the momenta can be determined with high precision, one usually focuses on the semi-leptonic decay of the t (corresponding to the leptonic decay of the W^+), for spin analysis.

Since the values of κ_f in eq. (2.3) follow from the $V-A$ structure of the $Wf\bar{f}'$ couplings, it is important to consider how they are affected by a nonzero anomalous tbW^+ coupling. New physics may appear in the tbW decay vertex, apart from that in top production, leading to changed decay width and distributions for the W^+ and l^+ . A model-independent form for the tbW vertex can be written as

$$\Gamma^\mu = \frac{-ig}{\sqrt{2}} \left[\gamma^\mu (f_{1L} P_L + f_{1R} P_R) - \frac{i\sigma^{\mu\nu}}{m_W} (p_t - p_b)_\nu (f_{2L} P_L + f_{2R} P_R) \right] \quad (2.5)$$

where for the SM $f_{1L} = 1$ and the anomalous couplings $f_{1R} = f_{2L} = f_{2R} = 0$. Luckily, as has been shown in ref. [49] and will be discussed briefly below, it is precisely for the two best spin analyzers, the l^+ and the \bar{d} , that the value of κ_f in eq. (2.3) remains unchanged to leading order in the anomalous couplings. Hence this distribution is indeed a robust top spin analyzer.

So far we have discussed the somewhat academic issue of the correlation between the direction of the top spin, in an ensemble with degree of polarization P_t , and the angular distribution of the charged decay lepton. However, in an actual experiment we have to consider the process of top production and its semi-leptonic decay and perform the calculation preserving information on the top spin from production to decay. To this end, let us consider a generic process of top pair production and subsequent semi-leptonic decay of t and inclusive decay of \bar{t} , $AB \rightarrow t\bar{t} \rightarrow b\ell^+\nu_\ell X$. Since $\Gamma_t/m_t \sim 0.008$, we can use the narrow width approximation (NWA) to write the cross section as a product of the $2 \rightarrow 2$ production cross section times the decay width of the top. To preserve coherence of the top spin in production and decay, we need to use the spin density matrix formalism. The

amplitude squared can be factored into production and decay parts in the NWA [49]:

$$\overline{|\mathcal{M}|^2} = \frac{\pi\delta(p_t^2 - m_t^2)}{\Gamma_t m_t} \sum_{\lambda, \lambda'} \rho(\lambda, \lambda') \Gamma(\lambda, \lambda'). \quad (2.6)$$

where $\rho(\lambda, \lambda')$ and $\Gamma(\lambda, \lambda')$ are the 2×2 top production and decay spin density matrices respectively, with $\lambda, \lambda' = \pm 1$ denoting the top helicity. The phase space integrated $\rho(\lambda, \lambda')$ gives the polarization density matrix and can be parametrized as

$$\sigma(\lambda, \lambda') = \frac{\sigma_{\text{tot}}}{2} \begin{pmatrix} 1 + \eta_3 & \eta_1 - i\eta_2 \\ \eta_1 + i\eta_2 & 1 - \eta_3 \end{pmatrix}, \quad (2.7)$$

The (1,1) and (2,2) diagonal elements are the cross sections for the production of positive and negative helicity tops. $\sigma_{\text{tot}} = \sigma(+, +) + \sigma(-, -)$ gives the total cross section, whereas the difference $\sigma_{\text{pol}} = \sigma(+, +) - \sigma(-, -)$ is the polarization dependent part of the cross-section. In fact η_3 is the degree of *longitudinal* polarization and is given by the ratio of σ_{pol} to σ_{tot} as,

$$\eta_3 = P_t = \frac{\sigma(+, +) - \sigma(-, -)}{\sigma(+, +) + \sigma(-, -)} = \frac{\sigma_{\text{pol}}}{\sigma_{\text{tot}}}. \quad (2.8)$$

The production rates of the top with *transverse* polarization are given by the off-diagonal elements involving η_1 and η_2 , the two being the transverse components of the top polarization parallel and perpendicular to the production plane respectively. These are given by,

$$\eta_1 = \frac{\sigma(+, -) + \sigma(-, +)}{\sigma(+, +) + \sigma(-, -)}, \quad \eta_2 = \frac{\sigma(+, -) - \sigma(-, +)}{\sigma(+, +) + \sigma(-, -)}. \quad (2.9)$$

The spin dependence of the top decay is included via the top decay density matrix of eq. (2.6), $\Gamma(\lambda, \lambda')$. For the process $t \rightarrow bW^+ \rightarrow b\ell^+\nu_\ell$ this can be written in a Lorentz invariant form as

$$\Gamma(\pm, \pm) = \frac{2g^4}{|p_W^2 - m_W^2 + i\Gamma_W m_W|^2} (p_b \cdot p_\nu) [(p_\ell \cdot p_t) \mp m_t (p_\ell \cdot n_3)], \quad (2.10)$$

for the diagonal elements and

$$\Gamma(\mp, \pm) = -\frac{2g^4}{|p_W^2 - m_W^2 + i\Gamma_W m_W|^2} m_t (p_b \cdot p_\nu) p_\ell \cdot (n_1 \mp i n_2), \quad (2.11)$$

for the off-diagonal ones. Here the n_i^μ 's ($i = 1, 2, 3$) are the spin 4-vectors for the top with 4-momentum p_t , with the properties $n_i \cdot n_j = -\delta_{ij}$ and $n_i \cdot p_t = 0$. For decay in the rest frame they take the standard form $n_i^\mu = (0, \delta_i^k)$. As shown in [49], in the rest frame of the t quark the expression for $\Gamma(\lambda, \lambda')$, after phase space integration over the b quark and ν_ℓ momenta, factorizes into a lepton energy dependent part $F(E_\ell^0)$ and a function $A(\lambda, \lambda')$ which depends only on the angles of the decay lepton ℓ :

$$\langle \Gamma(\lambda, \lambda') \rangle = (m_t E_\ell^0) |\Delta(p_W^2)|^2 g^4 A(\lambda, \lambda') F(E_\ell^0). \quad (2.12)$$

Here angular brackets denote an average over the azimuthal angle of the b quark w.r.t the plane of the t and the ℓ momenta and $\Delta(p_W^2)$ stands for the propagator of the W . The

azimuthal correlation between b and ℓ is sensitive to new physics in the tbW couplings; this averaging eliminates any such dependence. Using the NWA for the top and the result of eq. (2.12) the differential cross section for top production and decay, after integrating over ν_ℓ and b , can be written as

$$d\sigma = \frac{1}{32 \Gamma_t m_t} \frac{1}{(2\pi)^4} \left[\sum_{\lambda, \lambda'} d\sigma(\lambda, \lambda') \times g^4 A(\lambda, \lambda') \right] |\Delta(p_W^2)|^2 \quad (2.13)$$

$$\times d \cos \theta_t d \cos \theta_\ell d\phi_\ell E_\ell F(E_\ell) dE_\ell dp_W^2.$$

As shown in [49], all three components of the top polarization, $\eta_i, i = 1, 3$, can be extracted by a suitable combination of lepton polar and azimuthal angular asymmetries, constructed by measuring the angular distributions of the decay lepton in the top rest frame. For example, as is expected from eq. (2.3), $\eta_3 = P_t$ is simply given by a forward backward asymmetry in the polar angle of the decay ℓ in the rest frame of the top, with the z axis along the top spin direction. Of course this requires reconstructing the top rest frame. As pointed out in the introduction, it would be interesting to devise variables for the decay lepton in the lab frame, which can be easily measured and are sensitive to top polarization.

The factorization of the $\langle \Gamma(\lambda, \lambda') \rangle$ of eq. (2.12) into $A(\lambda, \lambda')$, a function only of the polar and azimuthal angles of ℓ in the rest frame and $F(E_\ell^0)$ which is a function only of its energy E_ℓ^0 , is very significant. This factorization in fact leads to the result, mentioned already, viz. the energy averaged and normalized decay lepton angular distribution (and also for the \bar{d} quark), is independent of the anomalous tbW coupling to the linear order. This has been shown very generally for a $2 \rightarrow n$ process, using NWA for the top and neglecting terms quadratic in the anomalous couplings in (2.5) assuming new physics couplings to be small (for details see [49]). This thus implies that the charged lepton angular distribution eq. (2.14) is a very robust probe of top polarization, free from any possible modification of the tbW vertex due to new physics effect. Thus a measurement of top polarization via the angular observables of the decay lepton, gives us a pure probe of new physics in top production process alone. In contrast, the energy distributions of the l^+ or the angular distributions of the b and W may be “contaminated” by the anomalous tbW vertex, should the new physics being probed contribute to that as well.

In the next section we study the azimuthal distribution of the decay charged lepton from a top quark in $t\bar{t}$ pair production at the LHC in a model with Z' with chiral couplings. We then define an azimuthal asymmetry sensitive to top polarization using this distribution.

3 Results

We aim to investigate first the features of top polarization in the presence of a Z' resonance with chiral couplings. We will then examine the azimuthal distribution of charged leptons from top decay, and a certain azimuthal asymmetry to be defined later, as a probe of top polarization in the context of our chosen model.

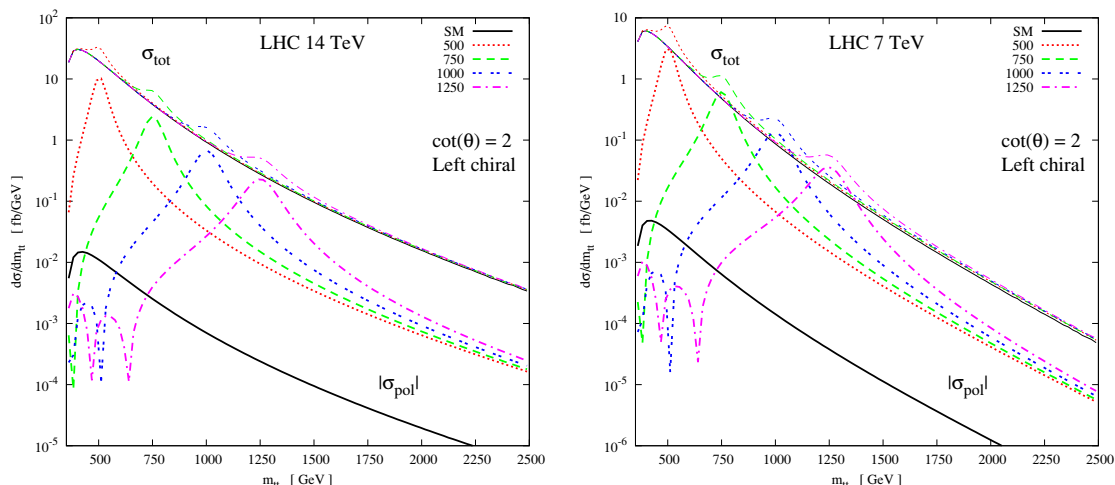


Figure 1. The $m_{t\bar{t}}$ distribution of total cross-section σ_{tot} (thin lines) and polarized part $|\sigma_{\text{pol}}|$ (thick lines) are shown for the SM (solid/black lines) and with Z' of mass 500 GeV (small-dashed/red lines), 750 GeV (long-dashed/green lines) 1000 GeV (double-dashed/blue lines) and 1250 GeV (dot-dashed/magenta lines) at 14 TeV LHC (left panel) and 7 TeV LHC (right panel). We have assumed $\cot(\theta) = 2$ and the left chiral couplings of Z' as in the Little Higgs model.

For our numerical calculations we use CTEQ6L1 parton distributions with a scale $Q = m_t = 175$ GeV. To account for non-leading order contributions, we assume the K -factor for the entire process to be the same as that for the SM $t\bar{t}$ production and thus use a value of 1.40 for LHC operating at $\sqrt{s} = 14$ TeV and 7 TeV ¹ and 1.08 for the Tevatron [59].

3.1 Top polarization

To get an idea of the longitudinal top polarization that the production of Z' may give rise to, we begin by calculating the distributions of σ_{tot} and σ_{pol} in the $t\bar{t}$ invariant mass $m_{t\bar{t}}$. Figure 1 shows these, including the Z' contribution for different Z' masses as well as the one expected for the SM, for the design value of \sqrt{s} of 14 TeV as well as its current value of 7 TeV.

Figure 1 shows that the distributions in the total cross-section peak at the respective Z' masses. Not only that, even the polarization dependent part peaks at the respective Z' masses, showing that the major contribution to the polarization comes from the chiral Z' coupling. On the other hand, the polarization dependent part of the cross section for the SM is lower by about 3 orders of magnitude. Since we calculate these distributions with left chiral couplings of Z' the polarized part is negative near the resonance, i.e. $\sigma(+, +) < \sigma(-, -)$. For sake of convenience, we plot the absolute value $|\sigma_{\text{pol}}|$ in figure 1. For the right chiral couplings the distribution is almost identical to that for the left chiral case, but with $\sigma(+, +) > \sigma(-, -)$ and is hence not shown. It is thus expected that at least in

¹We have checked using the tool HATHOR [58] that for CTEQ6M distributions the K -factor at $\sqrt{s} = 7$ TeV is the same as that for $\sqrt{s} = 14$ TeV. Hence we use the value of 1.40 for $\sqrt{s} = 7$ TeV in our case as well. It should be noted however, that since we construct asymmetries, those results will not depend on the assumed K -factor, except the ones on the sensitivity reach that is possible using these asymmetries.

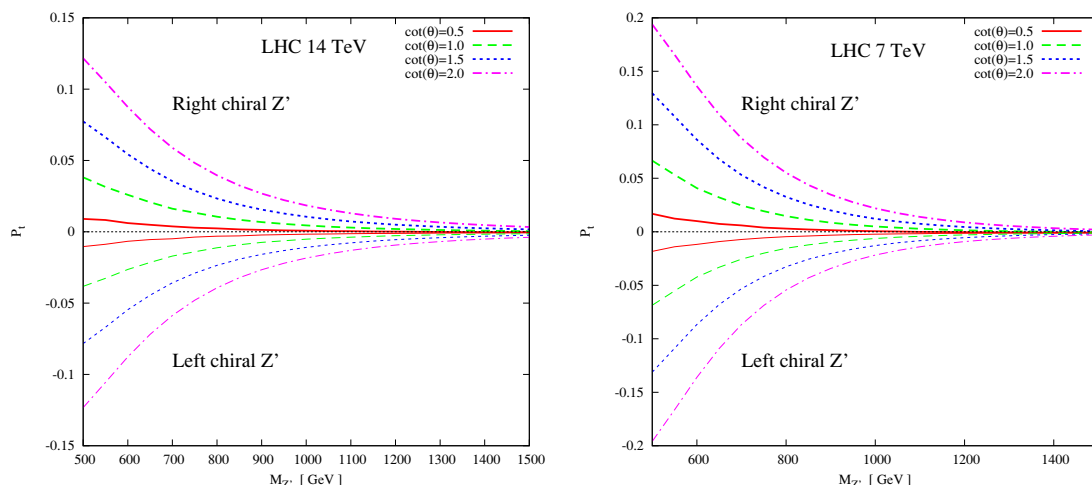


Figure 2. The $M_{Z'}$ dependence of the top polarization P_t for $\sqrt{s} = 14$ TeV (left panel) and $\sqrt{s} = 7$ TeV LHC (right panel). The thick lines are for the right-chiral coupling of Z' and the thin lines are for the left-chiral couplings. The curves are shown for $\cot(\theta) = 0.5$ (red/solid line), $\cot(\theta) = 1.0$ (green/big-dashed line), $\cot(\theta) = 1.5$ (blue/small-dashed line) and $\cot(\theta) = 2.0$ (magenta/dash-dotted line).

the region of the resonance, the top polarization would be a good measure of the chirality of the couplings.

Figure 1 also shows certain other interesting features, which do not directly concern us here. For example, sign changes in σ_{pol} arising when contributions with different s channel exchanges interfere show up as sharp dips in the distribution.

We also see that for $\sqrt{s} = 7$ TeV, $[\sigma(+,+) - \sigma(-,-)]_{Z'} > [\sigma(+,+) + \sigma(-,-)]_{SM}$ near the resonance, for $M_{Z'} \geq 750$ GeV. This means that in this case, it will be easier to distinguish the presence of Z' from the SM background than in the case of $\sqrt{s} = 14$ TeV. For the latter the increased and dominant $gg \rightarrow t\bar{t}$ contribution causes a reduction in the polarization of the top quark.

In figure 2 we show the degree of top polarization, $P_t = \sigma_{\text{pol}}/\sigma_{\text{tot}}$ as a function of $M_{Z'}$ for different values of the coupling $\cot(\theta)$ for $\sqrt{s} = 14$ and for $\sqrt{s} = 7$ TeV. Since the SM contribution to the top polarization coming from the off-shell Z boson is very small, $|P_t^{SM}| < 10^{-3}$ (see figure 1), we have not shown it. However, the full contribution from interference terms involving γ , Z and Z' exchanges is taken into account in all observables considered here. The relatively higher $q\bar{q}$ fluxes at the Tevatron, owing to it being a $p\bar{p}$ collider, and rather small gg flux because of its lower energy, leads to rather large values of expected top polarizations at the Tevatron, reaching 40%.

The top polarization in the presence of Z' is positive for right chiral couplings of Z' and negative for left chiral couplings. This is because the dominant contribution to the polarization comes for $m_{t\bar{t}}$ near Z' pole, where the top polarization is dictated by the chirality of its couplings. This suggests that a cut on $m_{t\bar{t}}$, like $|m_{t\bar{t}} - M_{Z'}| \leq 2\Gamma_{Z'}$ to select the Z' pole, will increase the net polarization of the top quark sample and also the sensitivity of any observable sensitive to the top polarization.

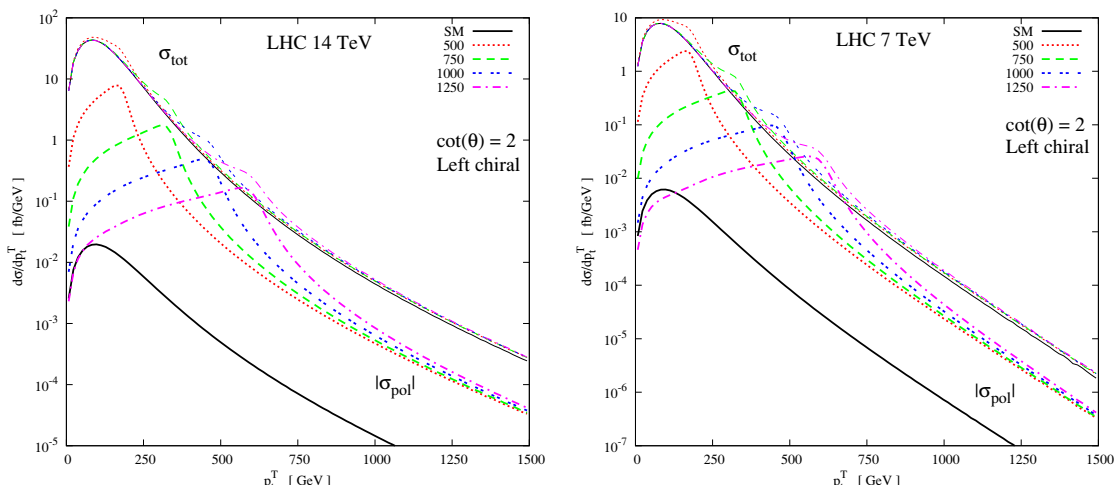


Figure 3. The p_t^T distribution for the unpolarized cross-section σ_{tot} (thin lines) and for the polarization dependent part $|\sigma_{\text{pol}}|$ (thick lines) for $\sqrt{s} = 14$ TeV (left panel) and $\sqrt{s} = 7$ TeV (right panel). The peak in the distribution occurs at $p_t^T = \beta_M M_{Z'}/2$ where $\beta_M = \sqrt{1 - 4m_t^2/M_{Z'}^2}$. The legend is the same as in figure 1.

Similarly, one can also look at the transverse momentum distribution of the top quark for signal enhancement. For a resonance of mass $M_{Z'}$ in the $t\bar{t}$ pair production, there is a peak at $m_{t\bar{t}} = M_{Z'}$ which translates to a peak in the transverse momentum at $p_t^T = \beta(M_{Z'}^2)M_{Z'}/2$, where $\beta(s) = \sqrt{1 - 4m_t^2/s}$. This peak is shown in the p_t^T distribution of total cross-section σ_{tot} and polarized part $|\sigma_{\text{pol}}|$ in figure 3. One can thus put a cut on the transverse momentum to improve the sensitivity of the polarization observables. The p_t^T cut will turn out to be useful, as we will see in the following sections.

We now study the use of the azimuthal distribution of the charged lepton coming from top decay as a tool to measure the top polarization.

3.2 Lepton azimuthal distribution

To define the azimuthal angle of the decay products of the top quark we choose the proton beam direction as the z axis and the top production plane as the $x - z$ plane, with top direction chosen to have positive x component. At the LHC, since the initial state has identical particles, the z -axis can point in the direction of either proton. This symmetry implies that one cannot distinguish between an azimuthal angle ϕ and an angle $2\pi - \phi$.

In figure 4 we compare the normalized distributions of the azimuthal angle ϕ_ℓ of the decay leptons calculated using eq. (2.14) for three cases, viz., (i) when the top quark has negligible polarization, $|P_t| \approx 10^{-3}$, as in the SM (black/solid line), (ii) when the top has 100% right-handed polarization, calculated keeping only the $\sigma(+, +)$ in eq. (2.14) (green/big-dashed line) and (iii) when the top has 100% left-handed polarization, calculated keeping only the $\sigma(-, -)$ in eq. (2.14) (blue/small-dashed line). As compared to the distribution for the (almost) unpolarized top in the SM, a positively polarized top leads to a distribution that is more sharply peaked near $\phi_\ell = 0$. The behaviour for a negatively

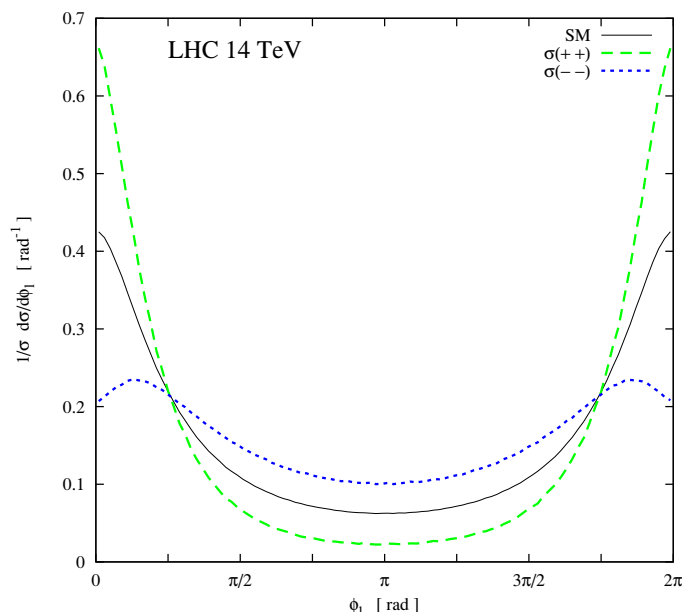


Figure 4. The normalized ϕ_ℓ distribution of the decay lepton for the SM: full contribution is shown in black/solid line, the positive helicity contribution from $\sigma(+, +)$ is shown in green/big-dashed line and the negative helicity contribution from $\sigma(-, -)$ is shown in blue/small-dashed line.

polarized top is opposite, and the relative number of leptons near $\phi_\ell = 0$ is far reduced. Thus, it is clear from the figure 4 that the azimuthal distribution can easily distinguish between 100% positive and 100% negative top polarizations. However, in practice, the produced top has partial polarization described by simultaneously non-zero values of $\sigma(+, +)$ as well as $\sigma(-, -)$ and also the spin-coherence contributions coming from the off-diagonal terms $\sigma(\pm, \mp)$.

The actual ϕ_ℓ distributions for $M_{Z'} = 500$ and 750 GeV with left and right chiral couplings, together with the SM distribution, are shown in figure 5. The figure clearly shows that for $M_{Z'} = 500$ GeV with right chiral couplings, which yields positive top polarization, there is greater peaking of the leptons near $\phi_\ell = 0$ as compared to the unpolarized SM distribution. Similarly, for left chiral couplings of the Z' corresponding to a negatively polarized top sample, the peak near $\phi_\ell = 0$ is reduced. In other words the qualitative behaviour of the ϕ_ℓ distribution for $M_{Z'} = 500$ GeV is same as for the completely polarized top quarks. This, however, is not the case for $M_{Z'} = 750$ GeV as can be seen from the right panel of figure 5.

To understand this observed change in the polarization dependence of the ϕ_ℓ distribution as we go from $M_{Z'} = 500$ GeV to a higher value of 750 GeV (as well as to understand its dependence on the top transverse momentum) we need to see how the ϕ_ℓ distribution in the laboratory frame is related to the simple angular distribution given in eq. (2.3) with $\kappa_f = 1$. The corresponding distribution in the laboratory frame, on using the relation

$$\cos \theta_\ell^* = \frac{\cos \theta_{t\ell} - \beta}{1 - \beta \cos \theta_{t\ell}} \tag{3.1}$$

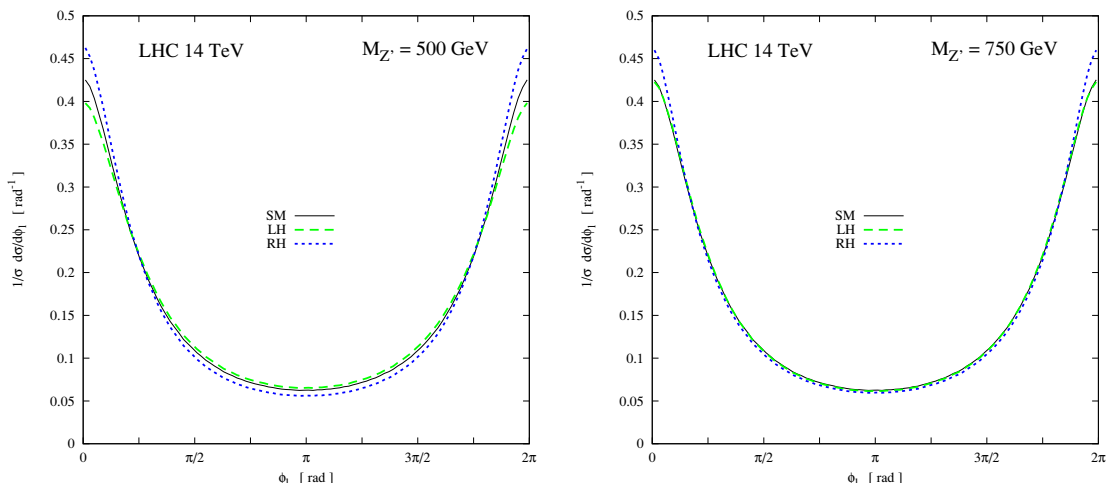


Figure 5. The ϕ_ℓ distribution of the decay lepton for the SM (black/solid line), Z' with left chiral (green/big-dashed line) and right chiral (blue/small-dashed line) couplings. No kinematical cut has been applied.

between the angle θ_ℓ^* between the top spin and the lepton direction in the rest frame of the top and the angle $\theta_{t\ell}$ between the top and lepton directions in the laboratory frame, becomes

$$\frac{1}{\Gamma_\ell} \frac{d\Gamma_\ell}{d \cos \theta_{t\ell}} = \frac{1}{2} (1 - \beta^2) (1 - P_t \beta) \frac{1 + \frac{P_t - \beta}{1 - P_t \beta} \cos \theta_{t\ell}}{(1 - \beta \cos \theta_{t\ell})^3}, \quad (3.2)$$

where $\beta = \sqrt{1 - m_t^2/E_t^2}$, and

$$\cos \theta_{t\ell} = \cos \theta_t \cos \theta_\ell + \sin \theta_t \sin \theta_\ell \cos \phi_\ell. \quad (3.3)$$

In practice, the distribution would also have to be integrated over θ_t , θ_ℓ and the lepton energy.

The first thing to note about the distribution of (3.2) is that because of the denominator, there is peaking for large $\cos \theta_{t\ell}$, and hence for small ϕ_ℓ , according to eq. (3.3). Thus, the boost produces a collimating effect along the direction of the top momentum, which gets translated to a peaking at $\phi_\ell = 0$. Secondly, unless $P_t = \pm 1$, the form of the distribution depends on relative values of P_t and typical values of β , in the combination

$$P_t^{\text{eff}} = \frac{P_t - \beta}{1 - P_t \beta}. \quad (3.4)$$

Thus there is a polarization dependent effect and an effect which occurs simply because of the boost, independent of the polarization, which could compete with each other. Thus, the dependence on ϕ_ℓ would turn out to be controlled by P_t so long as typical values of β are small compared to P_t . This condition would be satisfied for smaller values of E_t and hence of $M_{Z'}$, since the major contribution comes from $m_{t\bar{t}} \approx M_{Z'}$. This helps us to understand why, as mentioned earlier, the behaviour of the ϕ_l distribution is the same as that of completely polarized tops for $M_{Z'} = 500$ GeV, but not for $M_{Z'} = 750$ GeV. As we shall see, this will be useful in devising a suitable cut.

In the above reasoning, in order to illustrate the major effects of the change of frame from the top rest frame to the laboratory frame, we have taken a simplified approach, characterizing all top spin effects in terms of the longitudinal polarization P_t . In all our calculations, however, we deal with the full spin density matrix of the top quark, using eq. (2.6).

To characterize the shape of the ϕ_ℓ distribution, it is convenient to define a lepton azimuthal asymmetry [31, 50, 51]:

$$A_\ell = \frac{\sigma(\cos \phi_\ell > 0) - \sigma(\cos \phi_\ell < 0)}{\sigma(\cos \phi_\ell > 0) + \sigma(\cos \phi_\ell < 0)} = \frac{\sigma(\cos \phi_\ell > 0) - \sigma(\cos \phi_\ell < 0)}{\sigma_{\text{tot}}} . \quad (3.5)$$

This asymmetry is non-zero for the SM. While it is expected to be substantially different from the SM value of ~ 0.52 , when right chiral couplings of Z' are included, figure 5 indicates that for larger values of $M_{Z'}$, the asymmetry for left chiral couplings may not be very different from that for the SM.

In figure 6, left panel, we show the deviation δA_ℓ of the lepton azimuthal asymmetry from the SM value as a function of $M_{Z'}$ for different values of right and left chiral couplings. We see that while δA_ℓ can characterize well the polarization for the case of right chiral Z' couplings, it can discriminate left chiral couplings only for $M_{Z'}$ values below about 600 GeV. Ideally, we would like δA_ℓ to be a monotonic function of the top polarization for some choice of kinematics. In what follows, we investigate the possibility of finding suitable kinematical cuts, which when applied, makes $\delta A_\ell = A_\ell - A_\ell^{SM}$ a monotonically increasing function of the top polarization irrespective of the mass of Z' .

3.3 Kinematic cuts for A_ℓ

As can be seen from figures 1 and 3, the Z' resonance contributes to the unpolarized cross-section σ_{tot} and polarization σ_{pol} in the same kinematic region. In other words, there is a peak in the $m_{t\bar{t}}$ distribution at $m_{t\bar{t}}^{\text{pole}} = M_{Z'}$ and a peak in the p_t^T distribution at $(p_t^T)^{\text{peak}} = \beta(M_{Z'}^2)M_{Z'}/2$ for both σ_{tot} and σ_{pol} . Thus a cut on $m_{t\bar{t}}$ and/or p_t^T will help select the events with large top polarization and hence large contribution to A_ℓ . We study below the effects of these cuts on the shape of the ϕ_ℓ distribution and on the lepton asymmetry A_ℓ .

Since the Z' resonance appears at $m_{t\bar{t}} = M_{Z'}$, it is simple to imagine the importance of the $m_{t\bar{t}}$ cut. The p_t^T cut can be motivated as follows: As seen in figure 5 (right panel), the ϕ_ℓ distribution and hence the lepton asymmetry A_ℓ for the left chiral Z' is almost same as that of the SM. This happens because the left chiral Z' produces negatively polarized top quarks with high transverse momentum. Here the negative polarization tends to diminish the peaking near $\phi_\ell = 0$ of the leptons but the large transverse momentum of these highly polarized tops provides a larger factor of $\sin \theta_t$ in front of $\cos \phi_\ell$ in eq. (3.3), increasing the peaking, and the two effects can cancel each other. The kinematic effect always leads to collimation hence it only adds to the effect generated by positively polarized tops (right chiral Z'), while for negative top polarization it reduces the effect if not cancel it. If the transverse momentum of the top quark is too large then the kinematic effect may even over-compensate the de-collimating effect of the negative top quark polarization. On the other

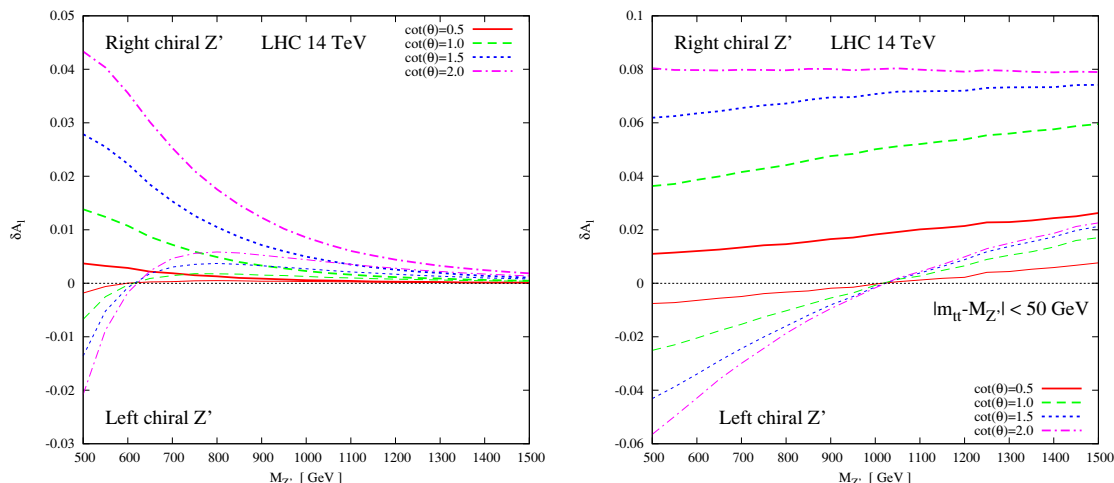


Figure 6. The δA_ℓ as a function of $M_{Z'}$ for $\cot(\theta) = 0.5$ (red/solid line), $\cot(\theta) = 1.0$ (green/big-dashed line), $\cot(\theta) = 1.5$ (blue/small-dashed line) and $\cot(\theta) = 2.0$ (magenta/dash-dotted line). The thick lines are for right chiral couplings and the thin lines are for left chiral couplings. The left panel is without any kinematical cut while for the right panel a cut $|m_{t\bar{t}} - M_{Z'}| < 50$ GeV is applied to enhance the Z' resonance effect.

hand, for the process under consideration the degree of polarization expected increases with a lower cut on p_t^T . Thus we need to choose a window of p_t^T values such that the contribution from Z' is maximized and δA_ℓ reflects the sign of the polarization

We have examined the effect of the following three kinds of kinematic cuts:

- **Resonant $m_{t\bar{t}}$ cut:** We select events with $m_{t\bar{t}}$ near $M_{Z'}$, i.e., $|m_{t\bar{t}} - M_{Z'}| < 50$ GeV for each value of $M_{Z'}$ and $\cot(\theta)$.
- **Fixed p_t^T cut:** We select events in a fixed range of the p_t^T for each value of $M_{Z'}$ and $\cot(\theta)$. Examples of this class of cuts chosen are $p_t^T > (p_t^T)^{\min}$, where $(p_t^T)^{\min} = 300, 400$ or 500 GeV.
- **Adaptive p_t^T cut:** We select events in a range of transverse momentum where the lower and the upper cuts depend both on the $M_{Z'}$ and $\cot(\theta)$ (via the decay width). One such cut is $p_t^T \in [\beta(M_{Z'}^2)(M_{Z'} - 2\Gamma_{Z'})/2, \beta(M_{Z'}^2)(M_{Z'} + 2\Gamma_{Z'})/2]$.

We show δA_ℓ as a function of $M_{Z'}$ and various values of $\cot(\theta)$, for both left and right chiral couplings, and without any kinematic cut, in the left panel of figure 6. As mentioned earlier, for $M_{Z'} < 600$ GeV the sign of δA_ℓ follows the chirality of the couplings and hence the sign of the top polarization. However, for larger masses and left chiral couplings of Z' , δA_ℓ changes sign because of the increased number of top events with large p_t^T . This, as mentioned earlier, over-compensates the de-collimation due to the negative polarization and leads to δA_ℓ having sign opposite to that of the polarization. Thus a measurement of δA_ℓ without any kinematic cut cannot determine even the sign of the top polarization, let alone its magnitude.

We first apply the resonant $m_{t\bar{t}}$ cut, i.e. $|m_{t\bar{t}} - M_{Z'}| < 50$ GeV and show the consequent δA_ℓ as a function of $M_{Z'}$ and various values of $\cot(\theta)$ in the right panel of figure 6 for both left and right chiral couplings. With a cut on the invariant mass near the resonance, the resultant top polarization is almost independent of $M_{Z'}$ when the decay width $\Gamma_{Z'}$ is larger than the range of the $m_{t\bar{t}}$ cut window, i.e., for $\cot(\theta) \geq 1.5$. The corresponding asymmetry too is almost independent of $M_{Z'}$ for the right chiral couplings. For the left chiral couplings, the asymmetry not only varies with $M_{Z'}$, it also changes its sign near $M_{Z'} = 1025$ GeV. Again, the change of sign is due to polarization independent collimation over compensating the de-collimation caused by negative polarization. Thus, even with the resonant selection cut on $m_{t\bar{t}}$ one cannot determine even the sign of the top polarization. The cut helps increase the net top polarization and thus the change of sign of δA_ℓ takes place at a higher value of the $M_{Z'}$ as compared to the previous case, shown in figure 6, left panel.

The next cut studied is the fixed p_t^T cut. We apply three different cuts: $p_t^T > 300, 400$ and 500 GeV and show δA_ℓ as a function of $M_{Z'}$ for different values of $\cot(\theta)$ in figure 7 top-left, top-right and bottom-left panels, respectively. We see that the sign of δA_ℓ follows the chirality of the Z' couplings for all three p_t^T cuts and also the curves for different values of $\cot(\theta)$ are ordered according to the values. In other words, with fixed p_t^T cuts δA_ℓ is a monotonically increasing function of $\cot(\theta)$ and hence that of top polarization.

This is not so for the third cut, the adaptive p_t^T cut shown in the bottom-right panel of figure 7. In this case the width of the window depends upon $\cot(\theta)$ through $\Gamma_{Z'}$. Thus for different values of $\cot(\theta)$, the amount of QCD $t\bar{t}$ production included in the denominator in the calculation of asymmetry differs. This explains why the curve for $\cot(\theta) = 2.0$ crosses the curve for $\cot(\theta) = 1.5$ for left chiral Z' with adaptive cuts. But this mostly reflects the somewhat higher effective value of the polarization that is attained even for a lower value of $\cot(\theta)$.

As for the shapes of the δA_ℓ curves for fixed p_t^T cuts, we note that there is a peak in the p_t^T distribution for $(p_t^T)^{peak} = \beta(M_{Z'}^2)M_{Z'}/2$. For the $p_t^T > 300$ GeV cut (figure 7 top-left panel) the peak of the p_t^T distribution is removed for $M_{Z'} < 695$ GeV. The rise in $|\delta A_\ell|$ starts when the transverse momentum corresponding to $m_{t\bar{t}} = M_{Z'} + \Gamma_{Z'}$ appears above the cut, i.e. when we have $\beta((M_{Z'} + \Gamma_{Z'})^2)(M_{Z'} + \Gamma_{Z'})/2 > (p_t^T)^{min}$.

To summarize, we have motivated and numerically demonstrated the monotonic behaviour of δA_ℓ as a function of the longitudinal top polarization under fixed p_t^T cuts. In case of the adaptive p_t^T cut this is not as clear cut. We can say however that $p_t^T > 300$ GeV and the adaptive p_t^T cut are two suitable choices for studying the top polarizations. We shall use only these two cuts for other collider options in the later sections.

It is relevant to note here that a cut with $p_t^T > 400$ GeV or higher makes the decay product of the top quarks highly collimated and it may be difficult to extract the ϕ_ℓ distribution from such collimated final states. The problem in the case of adaptive p_t^T cut is more severe as the lower limit rises almost linearly with $M_{Z'}$. However, it has been reported [60] recently that reconstruction of the electron inside the fat top jet is possible up to $p_t^T \sim 1000$ GeV, and it may be possible to extract the ϕ_ℓ distribution with the help of sub-jet structure techniques even for heavy resonances with mass up to 2000 GeV. Alternatively, one can use observables [28] constructed out of energies of the decay products

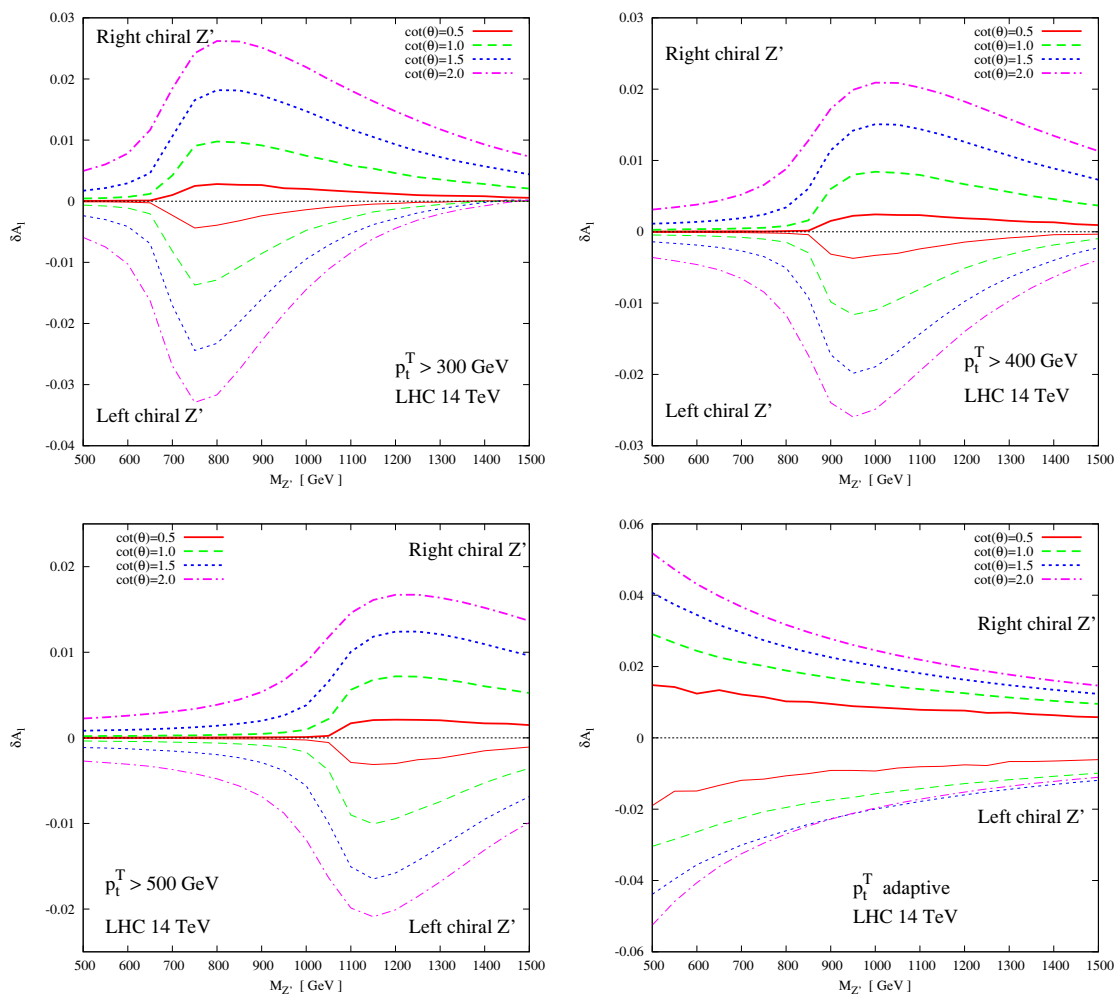


Figure 7. The δA_ℓ as a function of $M_{Z'}$ for $\cot(\theta) = 0.5$ (red/solid line), $\cot(\theta) = 1.0$ (green/big-dashed line), $\cot(\theta) = 1.5$ (blue/small-dashed line) and $\cot(\theta) = 2.0$ (magenta/dash-dotted line). The thick lines are for right chiral couplings and the thin lines are for left chiral couplings. The first three panels, from left to right and top to bottom, correspond to different values of the cut on p_t^T and the fourth panel corresponds to an adaptive p_t^T cut as described in the text.

in the case of highly boosted tops [61]. However, it must be remembered that some of these observables will not be as robust polarimeters as the lepton angular distribution, against the effect of anomalous couplings of the top.

3.4 Statistical significance of δA_ℓ

We now study the statistical significance of our chosen observable δA_ℓ under various conditions of \sqrt{s} and luminosity. For this we define the sensitivity for the observable δA_ℓ as:

$$\text{Sensitivity}(\delta A_\ell) = \frac{\delta A_\ell}{\Delta A_\ell^{SM}} = \frac{A_\ell - A_\ell^{SM}}{\Delta A_\ell^{SM}}, \quad \Delta A_\ell^{SM} = \sqrt{\frac{1 - (A_\ell^{SM})^2}{L \sigma_{\text{tot}}}} \quad (3.6)$$

The sensitivity defined above can be either positive or negative, depending on the sign of

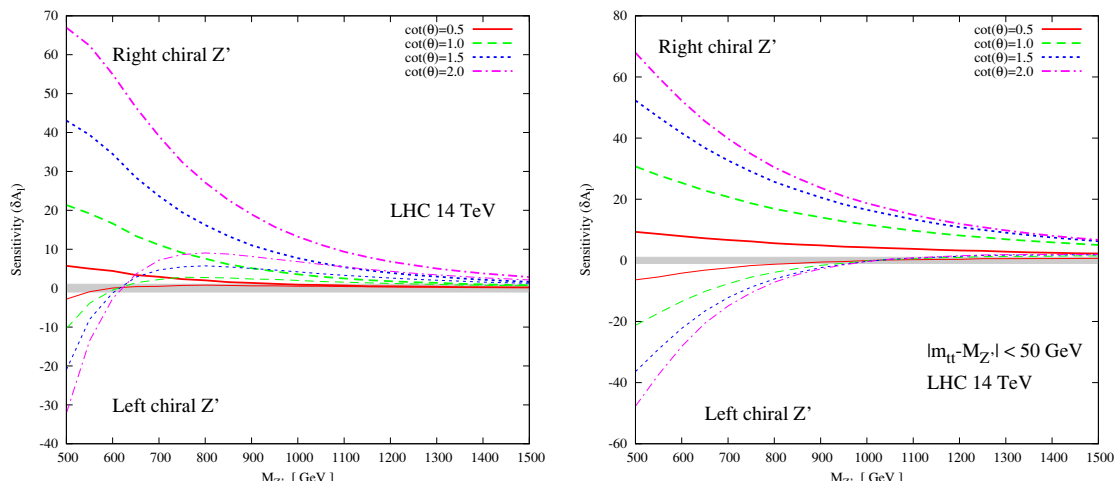


Figure 8. The sensitivity for δA_ℓ as a function of $M_{Z'}$ for $\sqrt{s} = 14$ TeV and integrated luminosity of 10 fb^{-1} ($\ell = e, \mu$). The shaded region corresponds to sensitivity between -1 and $+1$. The legend is the same as in figure 6.

δA_ℓ . If the value of the sensitivity lies between -1 and $+1$, the corresponding δA_ℓ would not be distinguishable at the 1σ level from the SM prediction. This region is shown shaded in the sensitivity plots. We show the sensitivities for $\sqrt{s} = 14$ TeV and an integrated luminosity of 10 fb^{-1} for the cases of no kinematic cut and the simple $m_{t\bar{t}}$ cut in figure 8. These sensitivities correspond to the asymmetries shown in figure 6. Similarly, in figure 9, we show the sensitivity for various p_t^T cuts corresponding to the asymmetries shown in the figure 7. For the right chiral Z' , the sensitivities are very large without any kinematical cuts. This means that the use of full set of events, without any cut, would be the best way to probe any new physics whose dynamics is expected to yield positive top polarizations [31]. For negative top polarizations, however, one needs to use kinematic cuts. For the present case of Z' the signal for negative top polarization can be enhanced with a cut on $m_{t\bar{t}}$ to select the resonance. This can be seen from figure 8 on comparing the sensitivities for left chiral Z' in the two panels. If, however, we want the asymmetry to tell us the sign of the top polarization correctly, we need to employ transverse momentum cuts. The corresponding sensitivities are also sizable for a large range of $M_{Z'}$ and $\cot(\theta)$ values. The best sensitivity, however, is achieved by means of an adaptive p_t^T cut. This cut requires a prior knowledge of the mass and some idea about the width of the resonance. Having this information at ones disposal one can use this cut to estimate the top polarization accurately once one has calibrated δA_ℓ against top polarization.

3.5 The role of kinematic cuts

We study here in some detail the effect of the kinematic cuts and how these lead to the monotonic behaviour of the azimuthal asymmetry with polarization, a property necessary for it to be a faithful probe of polarization.

To see the effect of the $m_{t\bar{t}}$ cut vis-à-vis the p_t^T cut we look at the ϕ_ℓ distribution for different $m_{t\bar{t}}$ and p_t^T slices for the SM and for Z' of a given mass with left or right

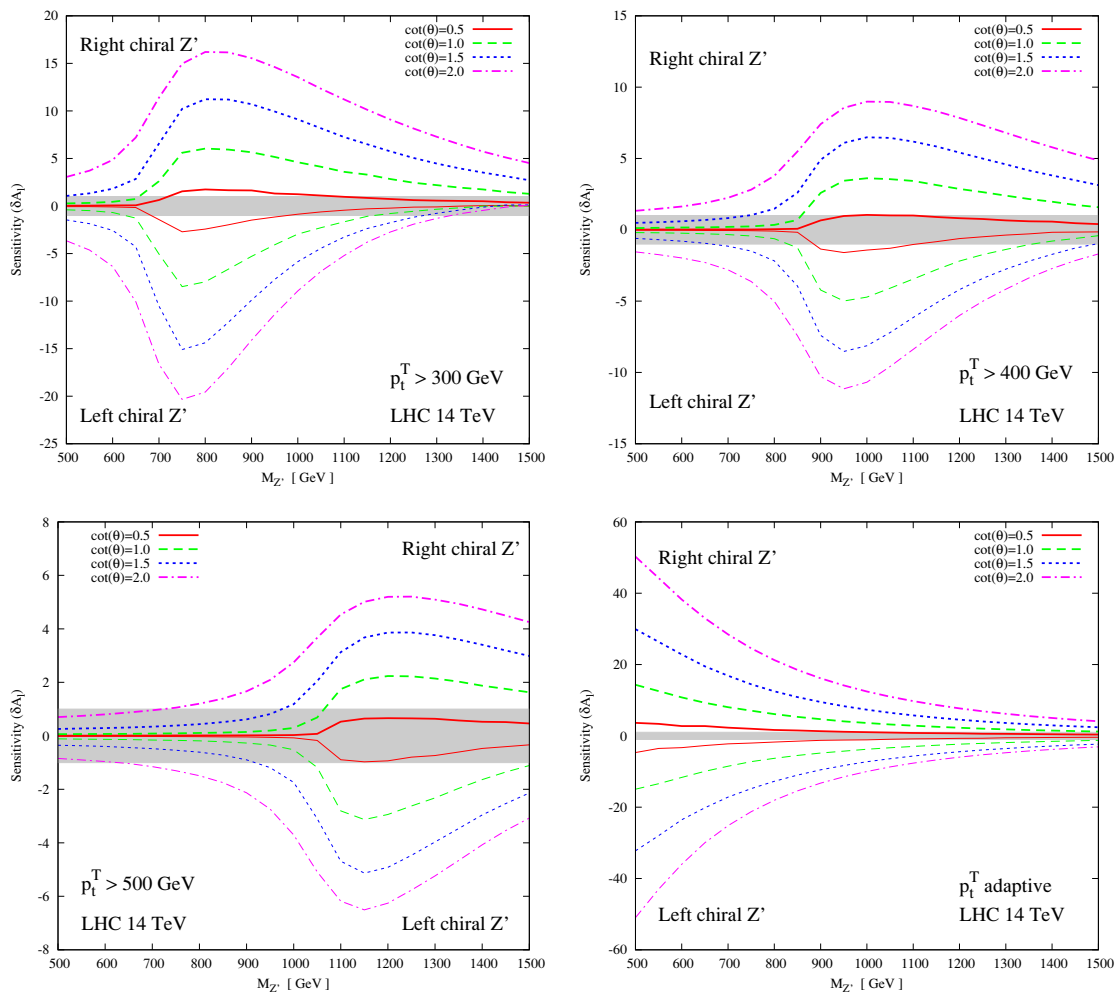


Figure 9. The sensitivity for δA_ℓ as a function of $M_{Z'}$ for $\sqrt{s} = 14$ TeV and integrated luminosity of 10 fb^{-1} ($\ell = e, \mu$). The shaded region corresponds to sensitivity between -1 and $+1$. The legend is same as in figure 7.

chiral couplings. These distributions, normalized to the rate in that slice, are shown in figure 10. Before we analyze these distributions it is instructive to note the relation between $m_{t\bar{t}}$ and p_t^T .

For a fixed $m_{t\bar{t}}$ the transverse momentum varies from 0 to a maximum value given by $(p_t^T)^{\text{max}} = \beta(m_{t\bar{t}}^2)m_{t\bar{t}}/2$. Thus each slice in $m_{t\bar{t}}$ is an average over this range of transverse momenta. Conversely, a given p_t^T slice corresponds to a range of invariant masses with a lower limit of $m_{t\bar{t}}^{\text{min}} = 2\sqrt{(p_t^T)^2 + m_t^2}$, but no upper limit.

In figure 10 (a), we show the ϕ_ℓ distributions for three different slices of $m_{t\bar{t}}$. The first one, $A \equiv m_{t\bar{t}} \in [350, 365] \text{ GeV}$, is the lowest slice near the threshold of the top pair production. Even for this slice the ϕ_ℓ distribution is not flat. This is due to the fact this slice contains a range of transverse momenta which can change the distribution. The second slice, B, is away from the threshold and also away from the Z' resonance. Thus

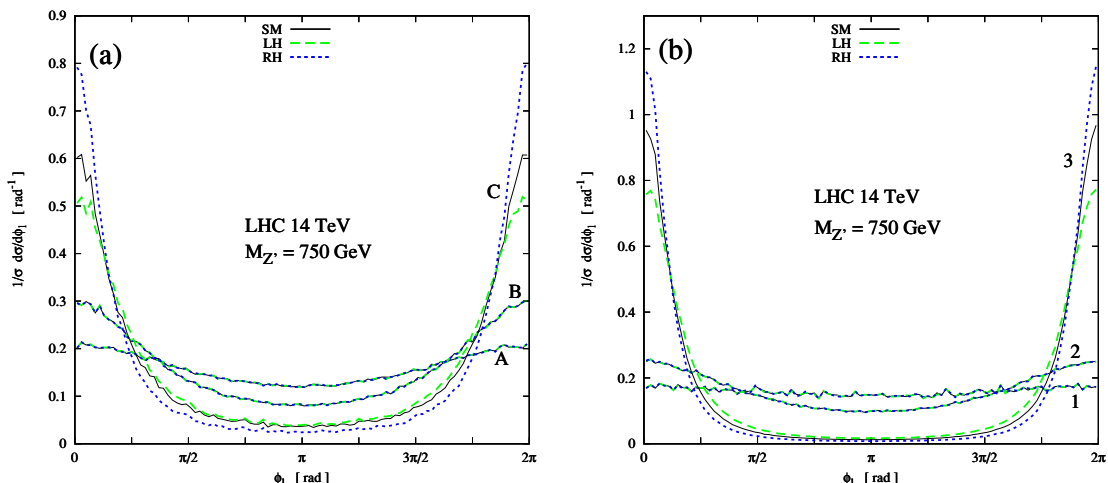


Figure 10. The normalized ϕ_ℓ distributions for for the SM and Z' of mass 750 GeV with both left and right chiral couplings (a) for three different $m_{t\bar{t}}$ slices, $A \equiv m_{t\bar{t}} \in [350, 365]$ GeV, $B \equiv m_{t\bar{t}} \in [395, 410]$ GeV, $C \equiv m_{t\bar{t}} \in [740, 755]$ GeV, and (b) for three p_t^T slices, $1 \equiv p_t^T \in [0, 15]$ GeV, $2 \equiv p_t^T \in [45, 60]$ GeV and $3 \equiv p_t^T \in [330, 345]$ GeV.

the slice B does not show any sign of polarization, i.e. curves for the SM and for both chirality of the Z' the normalized distribution are identical. In the slice C, which is near the Z' pole, there is large change in the ϕ_ℓ distribution owing to the large top polarization near the resonance. But since the slice C also contains events with a range of transverse momenta, this nice feature of the distribution may change if we look for heavier resonances. Already in the slice C the curves for left and right chiral Z' are not equidistant from the SM curves at $\phi_\ell = 0$, i.e. the transverse momentum dependent effect for the left chiral couplings is significant.

Next we look at figure 10 (b), which shows the ϕ_ℓ distributions for the same mass and couplings of Z' , but with different p_t^T slices. The slice “1” is the lowest p_t^T slice and the ϕ_ℓ distribution is flat owing to near zero polarization of the top sample and the near zero transverse momentum. The second slice “2” has slightly higher transverse momentum and it starts to show the collimation near $\phi_\ell = 0$ due to the effect of the transverse momentum. Since the top polarization for the slice “2” is also negligibly small, we have identical distributions for the SM and Z' with both chiralities. The slice “3” is near the peak in the p_t^T distribution corresponding to the Z' mass. Here we see a large collimation for all three cases due to large p_t^T , yet the effect of the top polarization is clearly visible. Also, the curves for left and right chiral Z' appear to be equidistant from the SM curve for $\phi_\ell = 0$. The lepton asymmetry for this case will be a monotonically increasing function of top polarization, as desired.

3.6 Results for lower energy colliders: the Tevatron and LHC with $\sqrt{s} = 7$ TeV

At present, both LHC and Tevatron are running. The LHC running at $\sqrt{s} = 7$ TeV, is expected to accumulate about 1 fb^{-1} integrated luminosity before upgrading to higher

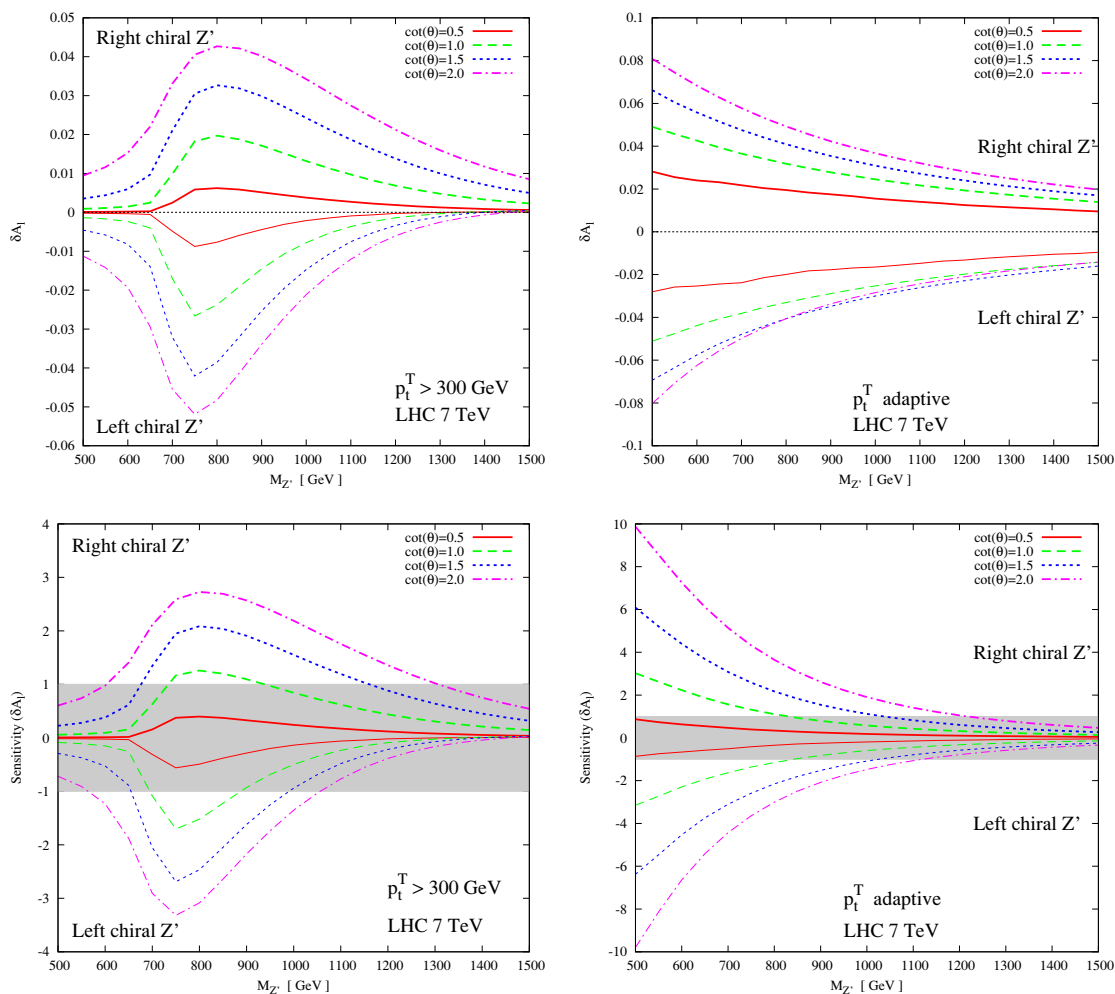


Figure 11. The asymmetry δA_ℓ as a function of $M_{Z'}$ at the LHC with $\sqrt{s} = 7 \text{ TeV}$ with different p_t^T cuts (top row) and the corresponding sensitivity (bottom row) for integrated luminosity 1 fb^{-1} ($l = e, \mu$). The shaded region corresponds to sensitivity between -1 and $+1$. The legend is the same as in figure 6.

energy. The Tevatron is expected to accumulate a total of 15 fb^{-1} before shutting down. Thus it will be instructive to look at the lepton asymmetry and corresponding sensitivities for these two collider options. For LHC at $\sqrt{s} = 7 \text{ TeV}$, we show the asymmetry δA_ℓ for two different cuts, fixed cut of $p_t^T > 300$ GeV and adaptive p_t^T cut in the top row of figure 11. The corresponding sensitivities are shown in the bottom row of the same figure. Similarly, figure 12 shows the asymmetry and the corresponding sensitivities for the Tevatron.

Due the lower energy and low luminosity at the $\sqrt{s} = 7 \text{ TeV}$ and $\int L dt = 1 \text{ fb}^{-1}$ run of the LHC, the sensitivity is 7 – 8 times smaller than that for the LHC at $\sqrt{s} = 14 \text{ TeV}$ and $\int L dt = 10 \text{ fb}^{-1}$. On the other hand, it is comparable to that for the Tevatron with $\int L dt = 15 \text{ fb}^{-1}$ with the fixed p_t^T cut and smaller than that for the Tevatron run for the adaptive p_t^T cut. The reason is that Tevatron being a $p\bar{p}$ machine, the $q\bar{q}$ luminosity is

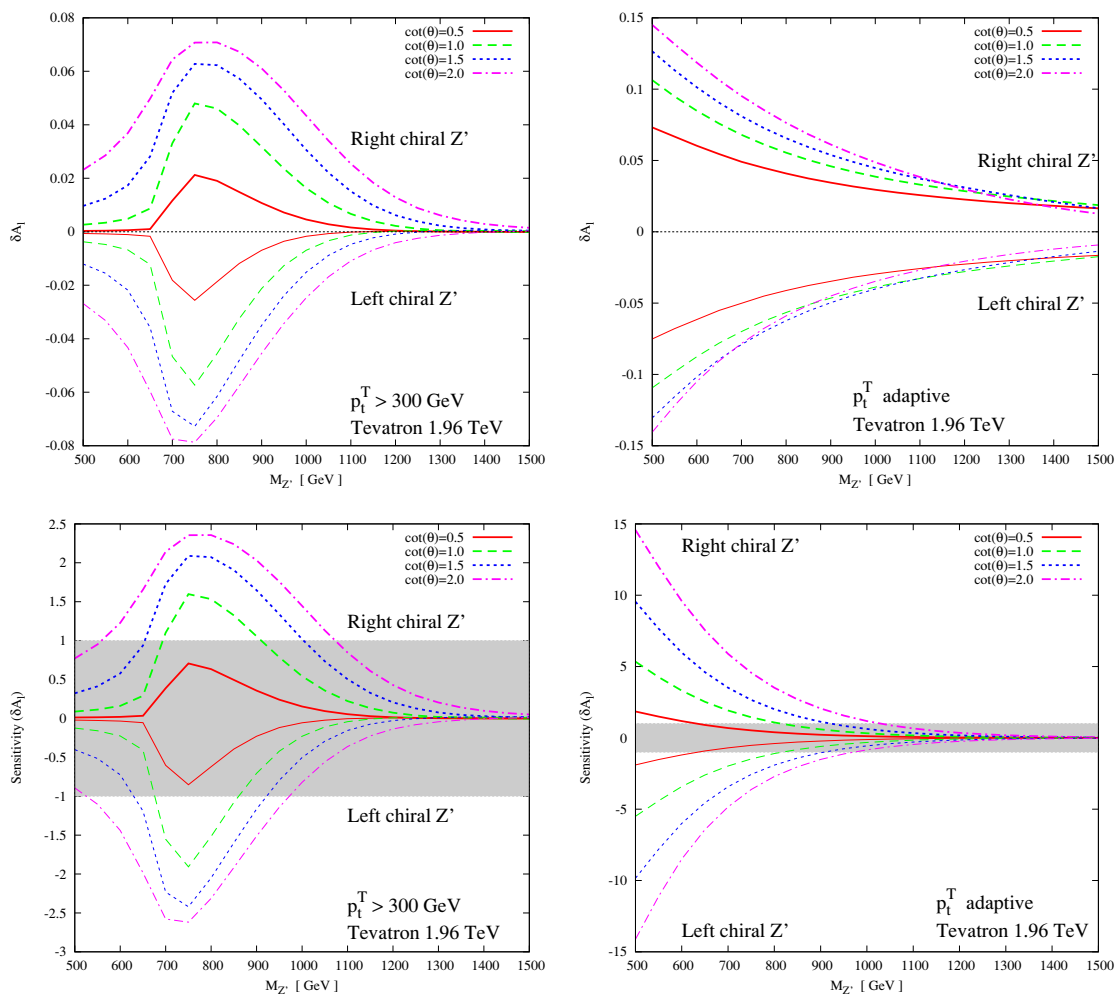


Figure 12. The asymmetry δA_ℓ as a function of $M_{Z'}$ at the Tevatron with $\sqrt{s} = 1.96$ TeV with different p_t^T cuts (top row) and the corresponding sensitivity (bottom row) for integrated luminosity of 15 fb^{-1} ($l = e, \mu$). The shaded region corresponds to sensitivity between -1 and $+1$. The legend is the same as in figure 6.

higher than at the LHC. Further, the lower energy of the Tevatron leads to a reduced background from $gg \rightarrow t\bar{t}$ as compared to the LHC 7 TeV run. Hence the Tevatron is more sensitive than LHC at $\sqrt{s} = 7$ TeV with the adaptive p_t^T cuts. It should be remembered that at the Tevatron the existence of a unique definition of the z axis, might offer us the possibility of constructing additional observables/asymmetries using the polar angle of the ℓ as well. This will be discussed elsewhere.

4 Conclusions

In this note we have investigated use of *single top polarization* as a probe of the $t\bar{t}$ production mechanism. To that end we have constructed an observable, which can reflect the sign and the magnitude of the top polarization faithfully. We do this by using the azimuthal

angle distribution of the decay lepton in the laboratory frame which carries information on the top-quark polarization. For purposes of illustration we have chosen a concrete model, inspired by the Little Higgs models, which has an additional spin-1 boson Z' with mass $M_{Z'}$ and chiral couplings to the quarks. In addition to the mass $M_{Z'}$, this model is characterized by one more parameter, $\cot(\theta)$ which gives the strength of the couplings. We began by studying the cross sections for producing a $t\bar{t}$ pair, where the top quark has a definite helicity (the cross-section being summed over the helicity state of the anti-top) and hence the degree of polarization of the produced top, as a function of the $t\bar{t}$ invariant mass $m_{t\bar{t}}$. We find that the top polarization dependent part of the cross section in the model can be large, even comparable to the unpolarized cross section, in the region of the Z' resonance. We also calculated the degree of top polarization in the model, and found it to be of the order of a few per cent for Z' masses around 1000 GeV, and larger for lower $M_{Z'}$ (for example it has a value $\sim 10\%$ for a Z' with mass 700 GeV for $\sqrt{s} = 7$ TeV) as compared to a value of less than 10^{-3} expected in the SM. The sign of the polarization follows the chirality of the Z' couplings to $t\bar{t}$. Further the polarization dependent part of the cross section was also found to peak in the region of the top-quark transverse momentum $p_t^T \approx \sqrt{1 - 4m_t^2/M_{Z'}^2} M_{Z'}/2$. Hence the t polarization can be maximized by appropriate cuts on $m_{t\bar{t}}$ or p_t^T .

We then investigated to what extent the azimuthal angular distribution of the charged lepton produced in top decay would mirror the extent of this large top polarization. It turned out that without any cuts, the normalized azimuthal distribution is sensitive to the magnitude and sign of the top polarization only for small $M_{Z'}$, up to about 600 GeV. The top polarization modifies the height of the peak that this distribution has near $\phi_\ell \approx 0$ (and $\phi_\ell \approx 2\pi$). The peak is higher (lower) for right (left) chiral couplings than for the SM: for example for $M_{Z'} = 500$ GeV a polarization of about 12% caused the peak to be higher by about 10%. This distribution is not symmetric in $\cos \phi_\ell$, and we can define an asymmetry A_ℓ about $\cos \phi_\ell = 0$. Since the initial state at the LHC has identical particles, choosing the beam axis as the z axis does not allow for a unique choice of the direction in which z is positive, leading to distributions which are symmetric under $\phi_\ell \rightarrow 2\pi - \phi_\ell$. This does not preclude, however, an asymmetry of the azimuthal distribution about $\cos \phi_\ell = 0$. A_ℓ has a nonzero value, A_ℓ^{SM} , for the SM, i.e. the case of an unpolarized top. The deviation of A_ℓ from its SM value, δA_ℓ , is sensitive to $\cot(\theta)$, as well as to the chirality of the Z' couplings for $M_{Z'} < 600$ GeV. We observe, however, that δA_ℓ becomes positive, for larger values of $M_{Z'}$, irrespective of the chirality. This indicates that the azimuthal distributions and asymmetry get contributions which are partly dependent on the top polarization, and partly purely kinematic in nature.

We then investigated effects of kinematic cuts in order to make the δA_ℓ more faithful to the sign and the magnitude of the t polarization, and hence to the couplings of the Z' , for a larger range of $M_{Z'}$. A cut on $m_{t\bar{t}}$ restricting it to the resonant region around $M_{Z'}$ makes the δA_ℓ independent of $M_{Z'}$, for the full range considered for right chiral couplings. Even though for the left chiral couplings this still happens only for a limited range of $M_{Z'}$, the range is now larger than without any cuts. Thus knowing the mass of the resonance

will already be of help. A cut on the top transverse momentum p_t^T restricting it to values larger than a fixed value of a few hundred GeV succeeds in getting δA_ℓ to reflect faithfully both the magnitude and the chirality of the coupling, alternatively magnitude and sign of the t polarization, irrespective of $M_{Z'}$. An adaptive cut, in which p_t^T is restricted to a window which depends on the width of Z' , and hence on the coupling $\cot(\theta)$, makes δA_ℓ more sensitive to lower values of $M_{Z'}$, even though not completely monotonic in $M_{Z'}$. Interestingly, now for the polarization values of a few per cent one gets δA_ℓ of the same order, and even enhanced by a factor of 2 – 3 by the adaptive p_t^T cut.

The statistical significance of the azimuthal asymmetry for various kinematic cuts was also examined, with the conclusion that the sensitivity is large for all values of $\cot(\theta) > 0.5$ that we consider. The best sensitivity is achieved with the use of the adaptive p_t^T cuts. As an example, for the design energy of the LHC of $\sqrt{s} = 14$ TeV and an integrated luminosity of 10 fb^{-1} , even with a plain cut on p_t^T we find sensitivity values ≥ 3 over a large part of the range of $M_{Z'}$ values considered, extending to large $M_{Z'}$.

We also evaluated the sensitivity of our observable for the current run of LHC with $\sqrt{s} = 7$ TeV and integrated luminosity of 1 fb^{-1} , as well as for the Tevatron with an integrated luminosity of 15 fb^{-1} . At $\sqrt{s} = 7$ TeV values of asymmetry δA_ℓ as high as 4–5% (6–7%) for a fixed (adaptive) p_t^T cut can be reached. Due to the smaller luminosity for this run, the sensitivity values are rather low and above 1σ only for $M_{Z'}$ values between 800 to 1200 GeV and for larger values of $\cot(\theta)$. It was found that the sensitivity at the Tevatron could be comparable to that at the LHC with $\sqrt{s} = 7$ TeV, though less than that at the 14 TeV version of the LHC.

In conclusion, the leptonic azimuthal asymmetry, with suitable cuts can be a useful tool for studying mechanisms for top production which can give rise to large spin-dependent effects.

Acknowledgments

R.G. wishes to acknowledge support from the Department of Science and Technology, India under Grant No. SR/S2/JCB-64/2007, under the J.C. Bose Fellowship scheme. K.R. gratefully acknowledges support from the Academy of Finland (Project No. 115032). S.D.R. thanks Helsinki Institute of Physics for hospitality during the period of completion of this work. The work of R.K.S has been supported by the German Ministry of Education and Research (BMBF) under contract no. 05H09WWE.

Open Access. This article is distributed under the terms of the Creative Commons Attribution Noncommercial License which permits any noncommercial use, distribution, and reproduction in any medium, provided the original author(s) and source are credited.

References

- [1] C.T. Hill and E.H. Simmons, *Strong dynamics and electroweak symmetry breaking*, *Phys. Rept.* **381** (2003) 235 [Erratum *ibid.* **390** (2004) 553] [[hep-ph/0203079](#)] [[SPIRES](#)].

- [2] M. Drees, R.M. Godbole and P. Roy, *Theory and phenomenology of sparticles*, World Scientific, Singapore (2005).
- [3] H. Baer and X. Tata, *Weak scale supersymmetry: from superfields to scattering events*, Cambridge University Press, Cambridge U.K. (2006).
- [4] N. Arkani-Hamed, A.G. Cohen and H. Georgi, *Twisted supersymmetry and the topology of theory space*, *JHEP* **07** (2002) 020 [[hep-th/0109082](#)] [[SPIRES](#)].
- [5] N. Arkani-Hamed, A.G. Cohen and H. Georgi, *Electroweak symmetry breaking from dimensional deconstruction*, *Phys. Lett. B* **513** (2001) 232 [[hep-ph/0105239](#)] [[SPIRES](#)].
- [6] P.H. Frampton and S.L. Glashow, *Chiral color: an alternative to the standard model*, *Phys. Lett. B* **190** (1987) 157 [[SPIRES](#)].
- [7] P.H. Frampton and S.L. Glashow, *Unifiable chiral color with natural gim mechanism*, *Phys. Rev. Lett.* **58** (1987) 2168 [[SPIRES](#)].
- [8] R.S. Chivukula, A.G. Cohen and E.H. Simmons, *New strong interactions at the Tevatron?*, *Phys. Lett. B* **380** (1996) 92 [[hep-ph/9603311](#)] [[SPIRES](#)].
- [9] L. Randall and R. Sundrum, *A large mass hierarchy from a small extra dimension*, *Phys. Rev. Lett.* **83** (1999) 3370 [[hep-ph/9905221](#)] [[SPIRES](#)].
- [10] C. Kilic, T. Okui and R. Sundrum, *Colored resonances at the Tevatron: phenomenology and discovery potential in multijets*, *JHEP* **07** (2008) 038 [[arXiv:0802.2568](#)] [[SPIRES](#)].
- [11] M. Beneke et al., *Top quark physics*, [hep-ph/0003033](#) [[SPIRES](#)].
- [12] W. Bernreuther, *Top quark physics at the LHC*, *J. Phys. G* **35** (2008) 083001 [[arXiv:0805.1333](#)] [[SPIRES](#)].
- [13] T. Han, *The ‘top priority’ at the LHC*, *Int. J. Mod. Phys. A* **23** (2008) 4107 [[arXiv:0804.3178](#)] [[SPIRES](#)].
- [14] R. Frederix and F. Maltoni, *Top pair invariant mass distribution: a window on new physics*, *JHEP* **01** (2009) 047 [[arXiv:0712.2355](#)] [[SPIRES](#)].
- [15] CDF collaboration, T. Aaltonen et al., *Search for resonant $t\bar{t}$ production in $p\bar{p}$ collisions at $\sqrt{s} = 1.96$ TeV*, *Phys. Rev. Lett.* **100** (2008) 231801 [[arXiv:0709.0705](#)] [[SPIRES](#)].
- [16] CDF collaboration, T. Aaltonen et al., *Limits on the production of narrow $t\bar{t}$ resonances in $p\bar{p}$ collisions at $\sqrt{s} = 1.96$ TeV*, *Phys. Rev. D* **77** (2008) 051102 [[arXiv:0710.5335](#)] [[SPIRES](#)].
- [17] D0 collaboration, V.M. Abazov et al., *Search for $t\bar{t}$ resonances in the lepton plus jets final state in $p\bar{p}$ collisions at $\sqrt{s} = 1.96$ TeV*, *Phys. Lett. B* **668** (2008) 98 [[arXiv:0804.3664](#)] [[SPIRES](#)].
- [18] CDF collaboration, T. Aaltonen et al., *Search for new color-octet vector particle decaying to $t\bar{t}$ in $p\bar{p}$ collisions at $\sqrt{s} = 1.96$ TeV*, *Phys. Lett. B* **691** (2010) 183 [[arXiv:0911.3112](#)] [[SPIRES](#)].
- [19] M. Guchait, F. Mahmoudi and K. Sridhar, *Tevatron constraint on the Kaluza-Klein gluon of the bulk Randall-Sundrum model*, *JHEP* **05** (2007) 103 [[hep-ph/0703060](#)] [[SPIRES](#)].
- [20] D. Choudhury, R.M. Godbole, R.K. Singh and K. Wagh, *Top production at the Tevatron/LHC and nonstandard, strongly interacting spin one particles*, *Phys. Lett. B* **657** (2007) 69 [[arXiv:0705.1499](#)] [[SPIRES](#)].
- [21] D0 collaboration, V.M. Abazov et al., *First measurement of the forward-backward charge asymmetry in top quark pair production*, *Phys. Rev. Lett.* **100** (2008) 142002 [[arXiv:0712.0851](#)] [[SPIRES](#)].

- [22] CDF collaboration, T. Aaltonen et al., *Forward-backward asymmetry in top quark production in $p\bar{p}$ collisions at $\sqrt{s} = 1.96$ TeV*, *Phys. Rev. Lett.* **101** (2008) 202001 [[arXiv:0806.2472](#)] [[SPIRES](#)].
- [23] E. Boos et al., *Polarisation in sfermion decays: determining $\tan\beta$ and trilinear couplings*, *Eur. Phys. J. C* **30** (2003) 395 [[hep-ph/0303110](#)] [[SPIRES](#)].
- [24] T. Gajdosik, R.M. Godbole and S. Kraml, *Fermion polarization in sfermion decays as a probe of CP phases in the MSSM*, *JHEP* **09** (2004) 051 [[hep-ph/0405167](#)] [[SPIRES](#)].
- [25] K.-i. Hikasa, J.M. Yang and B.-L. Young, *R-parity violation and top quark polarization at the Fermilab Tevatron collider*, *Phys. Rev. D* **60** (1999) 114041 [[hep-ph/9908231](#)] [[SPIRES](#)].
- [26] M. Arai, K. Huitu, S.K. Rai and K. Rao, *Single production of sleptons with polarized tops at the Large Hadron Collider*, *JHEP* **08** (2010) 082 [[arXiv:1003.4708](#)] [[SPIRES](#)].
- [27] M. Perelstein and A. Weiler, *Polarized tops from stop decays at the LHC*, *JHEP* **03** (2009) 141 [[arXiv:0811.1024](#)] [[SPIRES](#)].
- [28] J. Shelton, *Polarized tops from new physics: signals and observables*, *Phys. Rev. D* **79** (2009) 014032 [[arXiv:0811.0569](#)] [[SPIRES](#)].
- [29] M.M. Nojiri and M. Takeuchi, *Study of the top reconstruction in top-partner events at the LHC*, *JHEP* **10** (2008) 025 [[arXiv:0802.4142](#)] [[SPIRES](#)].
- [30] K. Agashe, A. Belyaev, T. Krupovnickas, G. Perez and J. Virzi, *LHC signals from warped extra dimensions*, *Phys. Rev. D* **77** (2008) 015003 [[hep-ph/0612015](#)] [[SPIRES](#)].
- [31] A. Djouadi, G. Moreau and R.K. Singh, *Kaluza–Klein excitations of gauge bosons at the LHC*, *Nucl. Phys. B* **797** (2008) 1 [[arXiv:0706.4191](#)] [[SPIRES](#)].
- [32] P.S. Bhupal Dev, A. Djouadi, R.M. Godbole, M.M. Muhlleitner and S.D. Rindani, *Determining the CP properties of the Higgs boson*, *Phys. Rev. Lett.* **100** (2008) 051801 [[arXiv:0707.2878](#)] [[SPIRES](#)].
- [33] G. Mahlon and S.J. Parke, *Angular correlations in top quark pair production and decay at hadron colliders*, *Phys. Rev. D* **53** (1996) 4886 [[hep-ph/9512264](#)] [[SPIRES](#)].
- [34] G. Mahlon and S.J. Parke, *Maximizing spin correlations in top quark pair production at the Tevatron*, *Phys. Lett. B* **411** (1997) 173 [[hep-ph/9706304](#)] [[SPIRES](#)].
- [35] G. Mahlon and S.J. Parke, *Spin correlation effects in top quark pair production at the LHC*, *Phys. Rev. D* **81** (2010) 074024 [[arXiv:1001.3422](#)].
- [36] T. Stelzer and S. Willenbrock, *Spin correlation in top-quark production at hadron colliders*, *Phys. Lett. B* **374** (1996) 169 [[hep-ph/9512292](#)] [[SPIRES](#)].
- [37] W. Bernreuther, A. Brandenburg, Z.G. Si and P. Uwer, *Top quark spin correlations at hadron colliders: Predictions at next-to-leading order QCD*, *Phys. Rev. Lett.* **87** (2001) 242002 [[hep-ph/0107086](#)] [[SPIRES](#)].
- [38] W. Bernreuther, A. Brandenburg, Z.G. Si and P. Uwer, *Top quark pair production and decay at hadron colliders*, *Nucl. Phys. B* **690** (2004) 81 [[hep-ph/0403035](#)] [[SPIRES](#)].
- [39] W. Bernreuther and Z.G. Si, *Distributions and correlations for top quark pair production and decay at the Tevatron and LHC*, *Nucl. Phys. B* **837** (2010) 90 [[arXiv:1003.3926](#)] [[SPIRES](#)].
- [40] M. Arai, N. Okada, K. Smolek and V. Simak, *Top quark spin correlations in the Randall-Sundrum model at the CERN Large Hadron Collider*, *Phys. Rev. D* **75** (2007) 095008 [[hep-ph/0701155](#)] [[SPIRES](#)].
- [41] B. Grzadkowski and Z. Hioki, *New hints for testing anomalous top quark interactions at future linear colliders*, *Phys. Lett. B* **476** (2000) 87.

- [42] B. Grzadkowski and Z. Hioki, *Decoupling of anomalous top-decay vertices in angular distribution of secondary particles*, *Phys. Lett. B* **557** (2003) 55 [[hep-ph/0208079](#)] [[SPIRES](#)].
- [43] Z. Hioki, *A New decoupling theorem in top quark physics*, [hep-ph/0210224](#) [[SPIRES](#)].
- [44] Z. Hioki, *Probing anomalous top couplings through the final lepton angular and energy distributions at polarized NLC*, [hep-ph/0104105](#) [[SPIRES](#)].
- [45] K. Ohkuma, *Effects of top-quark anomalous decay couplings at $\gamma\gamma$ colliders*, *Nucl. Phys. (Proc. Suppl.) B* **111** (2002) 285.
- [46] B. Grzadkowski and Z. Hioki, *Angular distribution of leptons in general $t\bar{t}$ production and decay*, *Phys. Lett. B* **529** (2002) 82 [[hep-ph/0112361](#)] [[SPIRES](#)].
- [47] S.D. Rindani, *Effect of anomalous tbW vertex on decay-lepton distributions in $e^+e^- \rightarrow t\bar{t}$ and CP-violating asymmetries*, *Pramana* **54** (2000) 791 [[hep-ph/0002006](#)] [[SPIRES](#)].
- [48] R.M. Godbole, S.D. Rindani and R.K. Singh, *Study of CP property of the Higgs at a photon collider using $\gamma\gamma \rightarrow t\bar{t} \rightarrow lX$* , *Phys. Rev. D* **67** (2003) 095009 [Erratum *ibid.* **D 71** (2005) 039902] [[hep-ph/0211136](#)] [[SPIRES](#)].
- [49] R.M. Godbole, S.D. Rindani and R.K. Singh, *Lepton distribution as a probe of new physics in production and decay of the t quark and its polarization*, *JHEP* **12** (2006) 021 [[hep-ph/0605100](#)] [[SPIRES](#)].
- [50] B.C. Allanach et al., *Les Houches ‘Physics at TeV colliders 2005’ beyond the standard model working group: summary report*, [hep-ph/0602198](#) [[SPIRES](#)].
- [51] R.M. Godbole, S.D. Rindani, K. Rao and R.K. Singh, *Top polarization as a probe of new physics*, *AIP Conf. Proc.* **1200** (2010) 682 [[arXiv:0911.3622](#)] [[SPIRES](#)].
- [52] P. Langacker, *The physics of heavy Z' gauge bosons*, *Rev. Mod. Phys.* **81** (2009) 1199 [[arXiv:0801.1345](#)] [[SPIRES](#)].
- [53] P. Langacker, *Z' physics at the LHC*, [arXiv:0911.4294](#) [[SPIRES](#)].
- [54] E. Salvioni, A. Strumia, G. Villadoro and F. Zwirner, *Non-universal minimal Z' models: present bounds and early LHC reach*, *JHEP* **03** (2010) 010 [[arXiv:0911.1450](#)] [[SPIRES](#)].
- [55] E. Salvioni, G. Villadoro and F. Zwirner, *Minimal Z' models: present bounds and early LHC reach*, *JHEP* **11** (2009) 068 [[arXiv:0909.1320](#)] [[SPIRES](#)].
- [56] PARTICLE DATA GROUP collaboration, C. Amsler et al., *Review of particle physics*, *Phys. Lett. B* **667** (2008) 1 [[SPIRES](#)].
- [57] T. Han, H.E. Logan, B. McElrath and L.-T. Wang, *Phenomenology of the little Higgs model*, *Phys. Rev. D* **67** (2003) 095004 [[hep-ph/0301040](#)] [[SPIRES](#)].
- [58] M. Aliev et al., *HATHOR – HAdronic Top and Heavy quarks crOss section calculator*, [arXiv:1007.1327](#) [[SPIRES](#)].
- [59] J.M. Campbell, J.W. Huston and W.J. Stirling, *Hard interactions of quarks and gluons: a primer for LHC physics*, *Rept. Prog. Phys.* **70** (2007) 89 [[hep-ph/0611148](#)] [[SPIRES](#)].
- [60] ATLAS collaboration, *Prospects for top anti-top resonance searches using early ATLAS data*, [ATL-PHYS-PUB-2010-008](#).
- [61] D. Krohn, J. Shelton and L.-T. Wang, *Measuring the polarization of boosted hadronic tops*, *JHEP* **07** (2010) 041 [[arXiv:0909.3855](#)] [[SPIRES](#)].